Conditional measurements as probes of quantum dynamics

Shabnam Siddiqui, Daniel Erenso, Reeta Vyas, and Surendra Singh
Department of Physics, University of Arkansas, Fayetteville, Arkansas 72701, USA
(Received 5 December 2002; published 17 June 2003)

We discuss conditional measurements as probes of quantum dynamics and show that they provide different ways to characterize quantum fluctuations. We illustrate this by considering the light from a subthreshold degenerate parametric oscillator. Analytic results and curves are presented to illustrate the behavior.

DOI: 10.1103/PhysRevA.67.063808 PACS number(s): 42.50.Dv, 42.50.Ar, 42.65.Ky

I. INTRODUCTION

Fluctuations are an integral feature of quantum dynamical evolution. For dissipative quantum optical sources, these fluctuations are reflected in the photoemissions from these sources. In this paper, we will use the terms photoemissions and photodetections interchangeably because photodetection is simply a matter of casting a net to catch the photons emitted by the source. A photoemission signals a fluctuation in progress. Hence, a conditional measurement that commences when a photoemission has occurred catches a fluctuation in the act and, in fact, allows us to observe the time evolution of the fluctuation [1]. This sort of information is not available in unconditioned measurements. Thus, conditional measurements allow us to probe quantum dynamics at a deeper level. Perhaps the best known example of conditional measurement is the measurement of the second-order intensity correlation that measures fluctuations of light intensity following a conditioning photodetection [2]. This is the basis of the observation of photon bunching or antibunching. Recently, measurements of quadrature squeezing conditioned on a photodetection have also been proposed and reported in cavity quantum electrodynamics [3,4]. In this paper, we consider conditional measurements in the context of parametric oscillators and show that such measurements provide sensitive probes of quantum dynamics and the language of conditional measurements provides powerful conceptual tools for unraveling and understanding nonclassical features of quantum dynamics [5–8].

Optical parametric oscillators (OPOs) and amplifiers [9] based on down-conversion have played a central role in the studies of nonclassical photon correlations and various schemes for quantum communication and computation [10]. The fundamental process in optical parametric oscillators is conversion of a pump photon of frequency ω_p into a pair of photons (signal and idler) of lower frequencies ω_s and ω_i in a nonlinear medium inside an optical cavity. The process conserves energy and momentum. Conservation of energy requires the pump and down-converted frequencies to be related by $\omega_p=\omega_s+\omega_i$ and conservation of momentum, also known as phase matching, requires the use of certain anisotropic material media and specific states of polarization for the pump, signal, and idler photons. If the down-converted photons have the same frequency ($\omega_s=\omega_i\equiv\omega_d$), polarization, and direction of propagation, the process is called degenerate otherwise it is called nondegenerate. In the former case, we speak of a degenerate parametric oscillator (DPO) and in the latter of a nondegenerate parametric oscillator.

We begin by considering a degenerate parametric oscillator in Sec. II and discuss conditional measurements of intensity and amplitude. Conditional measurements of quadrature fluctuations are discussed in Sec. III. We restrict our considerations to its operation below the threshold of sustained oscillations. This allows us to obtain simple analytic expressions for various quantities of interest. The results are summarized in Sec. IV.

II. CONDITIONAL MEASUREMENTS OF A DPO

The field from the DPO is governed by the interaction Hamiltonian for phase-matched down-conversion inside an optical cavity driven by a classical injected signal [5,6]. The equation of motion for the density operator $\hat{\rho}_d$ of the DPO field is then

$$\dot{\hat{\rho}}_d=\frac{\kappa\varepsilon}{2}[\hat{a}_d^{\dagger 2}-\hat{a}_d^2,\hat{\rho}_d]+\gamma(2\hat{a}_d\hat{\rho}_d\hat{a}_d^\dagger-\hat{a}_d^\dagger\hat{a}_d\hat{\rho}_d-\hat{\rho}_d\hat{a}_d^\dagger\hat{a}_d), \tag{1}$$

where κ is the mode-coupling constant, ε is the dimensionless amplitude of the classical pump field, γ is the cavity linewidth, and $\hat{a}_d$ and $\hat{a}_d^\dagger$ are the annihilation and creation operators for the DPO. In writing the equation of motion for the density matrix, we have neglected pump depletion that is a reasonable approximation for low down-conversion efficiencies and subthreshold operation of the DPO considered here. The combination $\kappa\varepsilon$ has been chosen to be real by a suitable definition of the phases of $\hat{a}_d$ and $\hat{a}_d^\dagger$.

Using the positive-P representation for the density matrix, we can map the equation of motion for the annihilation and creation operators for the DPO field onto a set of stochastic equations for the c-number amplitudes α_d and α_{d*} corresponding, respectively, to the annihilation and creation operators $\hat{a}$ and $\hat{a}_d$. These equations read [5,6]

$$\dot{\alpha}_d=-\gamma\alpha_d+\kappa\varepsilon\alpha_{d*}+\sqrt{\kappa\varepsilon}\xi_1(t), \tag{2}$$

$$\dot{\alpha}_{d*}=-\gamma\alpha_{d*}+\kappa\varepsilon\alpha_d+\sqrt{\kappa\varepsilon}\xi_2(t), \tag{3}$$

where $\xi_1(t)$ and $\xi_2(t)$ are two statistically independent real Gaussian white-noise processes with zero means and unit intensity. Normally ordered averages of $\hat{a}_d^\dagger$ and $\hat{a}_d$ can then be calculated by using the mapping

$$\langle :\hat{a}_d^{\dagger m}\hat{a}_d^n:\rangle \rightarrow \langle \alpha_{d*}^m \alpha_d^n\rangle, \tag{4}$$

where the averaging on the right-hand side is with respect to the positive-P function. Since the noise terms in Eqs. (2) and (3) are real, the variables α_d and α_{d*} can be chosen to be real. Then by using the simple transformation

$$\alpha_d = (u_1 + u_2), \quad \alpha_{d*} = (u_1 - u_2), \tag{5}$$

we find that the field produced by the DPO can be described in terms of two independent real Gaussian processes u_1 and u_2 with mean and correlation functions given by

$$\langle u_i\rangle = 0, \quad \langle u_i(t)u_j(t')\rangle = \delta_{ij}\frac{1}{4}\frac{\kappa\varepsilon}{\lambda_i}e^{-\lambda_i|t-t'|}, \tag{6}$$

where the decay constants λ_i are given by

$$\lambda_1 = \gamma - \kappa\varepsilon, \quad \lambda_2 = \gamma + \kappa\varepsilon. \tag{7}$$

Below threshold ($\kappa\varepsilon < \gamma$) both decay constants are positive. Higher-order correlations of u_1 and u_2, and therefore α_d and α_{d*}, can be expressed in terms of the second-order correlation function using the Gaussian moment theorem [11].

Using the result of Eq. (6), the steady-state mean values for the DPO field amplitude and its second-order moments are found to be [6]

$$\overline{a_d} \equiv \langle \hat{a}_d\rangle = 0 = \langle \hat{a}_d^\dagger\rangle \equiv \overline{a}_{d*}, \tag{8}$$

$$\overline{n_d} \equiv \langle \hat{n}_d\rangle = \frac{1}{2}\left[\frac{(\kappa\varepsilon/\gamma)^2}{1-(\kappa\varepsilon/\gamma)^2}\right], \tag{9}$$

$$\overline{a_d^2} \equiv \langle \hat{a}_d^2\rangle = \frac{\gamma}{\kappa\varepsilon}\overline{n_d} = \langle \hat{a}_d^{\dagger 2}\rangle \equiv \overline{a_{d*}^2}, \tag{10}$$

where $\hat{n}_d = \hat{a}_d^\dagger\hat{a}_d$ is the number operator for the DPO. In Eqs. (8)–(10) and in the rest of the paper, we denote the steady-state operator averages with a bar over the letter symbol for the operator. We see that the steady-state mean-field amplitude from the DPO vanishes. The contribution to the mean photon number is thus purely from quantum fluctuations. It should also be noted that since the mean values such as $\langle \hat{a}_d^2\rangle$ and $\langle \hat{a}_d^{\dagger 2}\rangle$ are nonvanishing, quantum fluctuations are not isotropic in phase. This phase dependent noise is the source of squeezing exhibited by the DPO. The steady-state mean photon number can be observed by measuring the mean intensity of the light emitted by the DPO and the mean-field amplitude can be measured in an interference experiment with a coherent field.

Before proceeding further, we recall that the intensity of light (photons/sec) from the DPO is related to the photon number inside the cavity by $\langle \hat{I}_d\rangle = 2\gamma\langle \hat{n}_d\rangle$. Because of this simple proportionality between the two, we will use the terms intensity and photon number interchangeably in the paper. In view of Eqs. (8)–(10), it follows that the steady-state intensity of the light from the DPO is proportional to the mean number of photons $\overline{n_d}$ inside the cavity and the mean amplitude of the field emitted by the DPO vanishes.

Let us now consider the intensity from the DPO at time $t = \tau$ following a photodetection in the steady state at $t = 0$. This intensity from the DPO, conditioned on a photodetection, is

$$I_{dd}(\tau) = 2\gamma\frac{\langle \hat{a}_d^\dagger(0)\hat{a}_d^\dagger(\tau)\hat{a}_d(\tau)\hat{a}_d(0)\rangle}{\langle \hat{n}_d(0)\rangle} = 2\gamma\frac{\langle :\hat{n}_d(0)\hat{n}_d(\tau):\rangle}{\langle \hat{n}_d(0)\rangle} \equiv 2\gamma n_{dd}(\tau), \tag{11}$$

where we have used the fact that the probability of a photodetection in the steady state is proportional to the steady-state intensity $2\gamma\langle \hat{n}_d\rangle = 2\gamma\overline{n_d}$ from the DPO. Thus, the conditioned intensity is proportional to the conditioned photon number. The conditioned intensity is related to the second-order intensity correlation function [2]

$$g_d^{(2)}(\tau) = \frac{\langle :\hat{n}_d(\tau)\hat{n}_d(0):\rangle}{\langle \hat{n}_d\rangle^2} = \frac{n_{dd}(\tau)}{\overline{n_d}}, \tag{12}$$

where the colons denote time and normal ordering of operators enclosed by them. From this equation, we see that the second-order intensity correlation function is the ratio of the conditioned photon number to the steady-state photon number.

The time dependence of conditioned photon number can be calculated with the help of Eqs. (5) and (6) to be

$$n_{dd}(\tau) = \overline{n_d} + \frac{1}{4}\left(\frac{\lambda_2}{\lambda_1}e^{-2\lambda_1\tau} + \frac{\lambda_1}{\lambda_2}e^{-2\lambda_2\tau}\right). \tag{13}$$

It can be seen that long after the first detection ($\tau \rightarrow \infty$), the mean photon number reverts to its steady-state value $\overline{n_d}$. The rate at which the system approaches the steady state is determined by λ_1 and λ_2 given by Eq. (7). Before $\tau = 0$, the mean photon number has its steady-state value $\overline{n_d}$. Immediately after a photodetection at $\tau = 0$, the mean photon number jumps from $\overline{n_d}$ to the value given by

$$n_{dd}(0) = \left(3\overline{n_d} + \frac{1}{2}\right), \tag{14}$$

and thereafter relaxes to the steady-state value $\overline{n_d}$ following Eq. (13). Conditioned photon number increases significantly compared to the steady-state value $\overline{n_d}$. This increase in the conditioned photon number, and therefore the conditioned mean intensity from the DPO, is even more pronounced far below threshold where $\overline{n_d} \ll 1$ (or $\kappa\varepsilon \ll \gamma$). The enhanced emission following a first photodetection can be understood by recalling that inside the DPO cavity photons are generated in pairs. Below threshold, the rate of pair generation is small so that the photons in each pair leak out from the cavity well before another pair is produced. Thus, although the mean number of photons in the cavity is very small, there are large fluctuations whenever a pump photon is down-converted into a pair of photons into the cavity mode. The detection of a first photon signals a fluctuation in progress which increases the mean number of photons in the cavity for a period of the

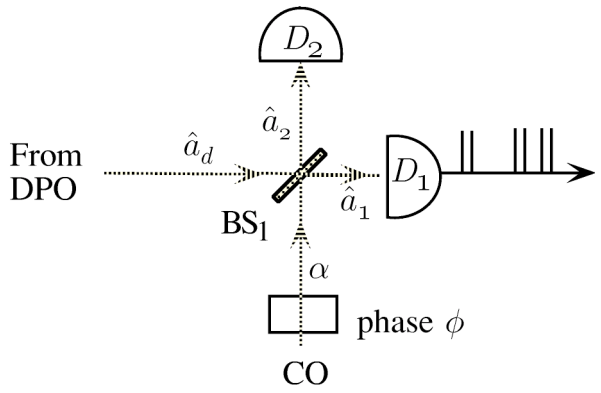

FIG. 1. An outline of the setup for detecting the interference of the light from the DPO with a coherent field. BS_1 is a lossless beam splitter and D_1 and D_2 are two photoelectric detectors that monitor the outputs at ports 1 and 2 of BS_1.

order of cavity lifetime $(2\gamma)^{-1}$. This increased mean photon number gives rise to enhanced emission from the cavity following a photodetection.

We also note that, such as the steady-state field amplitude $\bar{a}_d$, the conditional amplitude $\bar{a}_{dd}$ also vanishes indicating that the field from the DPO is incoherent. The emission from the DPO is thus pure noise and the contribution to its intensity is from incoherent fluctuations. These fluctuations, however, are not uniformly distributed in phase as we have already noted following Eqs. (8)–(10). The phase of the fluctuations can be observed in an interference experiment outlined in Fig. 1.

The light from the DPO is mixed with the light from a coherent oscillator (a laser with complex field amplitude $\alpha = |\alpha| e^{i\phi}$) at a loss-less beam splitter BS_1 of power reflectivity $\mathcal{R}$ and transmittivity $\mathcal{T}=1-\mathcal{R}$. The phase ϕ is relative to the classical pump for the DPO [6,12]. The superposed light in the two output modes, labeled by subscripts 1 and 2, of the beam splitter is detected by two photoelectric detectors D_1 and D_2, respectively. The annihilation operators for the two output modes can be written as [13]

$$\hat{a}_1 = \sqrt{\mathcal{R}}\alpha + \sqrt{\mathcal{T}}\hat{a}_d, \tag{15}$$

$$\hat{a}_2 = \sqrt{\mathcal{T}}\alpha - \sqrt{\mathcal{R}}\hat{a}_d. \tag{16}$$

Here, we have taken the beam splitter to be an antisymmetric beam splitter (for example, a glass plate with a silvered upper surface). Qualitatively no new features arise with other choices of beam splitters. We model the coherent oscillator (CO) field to be radiated by a laser operating high above threshold and take the linewidth of the laser cavity also to be γ. All measurements in the rest of this paper refer to the superposed fields given by Eqs. (15) and (16). Considering mode $\hat{a}_1$ for definiteness, we find its steady-state mean amplitude and intensity are given by

$$\bar{a}_1 \equiv \langle \hat{a}_1 \rangle = \sqrt{\mathcal{R}}\alpha + \sqrt{\mathcal{T}}\bar{a}_d = \sqrt{\mathcal{R}}\alpha, \tag{17}$$

$$\bar{n}_1 \equiv \langle \hat{n}_1 \rangle = \mathcal{R}\bar{n}_\alpha + \mathcal{T}\bar{n}_d + \sqrt{\mathcal{R}\mathcal{T}}(\alpha\bar{a}_d^* + \alpha^*\bar{a}_d) = \mathcal{R}\bar{n}_\alpha + \mathcal{T}\bar{n}_d. \tag{18}$$

From these equations, we see that the mean-field amplitude at port 1 has contribution only from the laser and that the mean photon number is the sum of contributions from the DPO and the laser. The interference term averages out to zero in the steady state.

Let us now consider conditional measurements. For definiteness we shall consider conditioning measurement to be a photodetection at port 1. Noting that the CO field remains unaffected by a photodetection, we can express the conditional expectation values of the superposed field variables in terms of the conditional expectation values of the DPO and CO field variables. Thus, the mean amplitude and intensity at port 1 conditioned on a detection at port 1 are [8]

$$a_{11}(\tau) \equiv \frac{\langle \hat{a}_1^\dagger(0)\hat{a}_1(\tau)\hat{a}_1(0)\rangle}{\langle \hat{n}_1 \rangle} = \sqrt{\mathcal{R}}\alpha + \sqrt{\mathcal{T}}a_{d1}(\tau), \tag{19}$$

$$\begin{aligned} a_{d1}(\tau) &\equiv \frac{\langle \hat{a}_1^\dagger(0)\hat{a}_d(\tau)\hat{a}_1(0)\rangle}{\langle \hat{n}_1 \rangle} \\ &= \frac{\kappa\varepsilon\sqrt{\mathcal{R}\mathcal{T}}}{4\bar{n}_1}\left[\left(\frac{e^{-\lambda_1\tau}}{\lambda_1} - \frac{e^{-\lambda_2\tau}}{\lambda_2}\right)\alpha \right. \\ &\quad \left. + \left(\frac{e^{-\lambda_1\tau}}{\lambda_1} + \frac{e^{-\lambda_2\tau}}{\lambda_2}\right)\alpha^*\right], \end{aligned} \tag{20}$$

$$\begin{aligned} n_{11}(\tau) &\equiv \frac{\langle \hat{a}_1^\dagger(0)\hat{n}_1(\tau)\hat{a}_1(0)\rangle}{\langle \hat{n}_1 \rangle} \\ &= \mathcal{R}\bar{n}_\alpha + \mathcal{T}n_{d1}(\tau) + \sqrt{\mathcal{R}\mathcal{T}}[\alpha a_{d1}^*(\tau) + \alpha^* a_{d1}(\tau)], \end{aligned} \tag{21}$$

$$\begin{aligned} n_{d1}(\tau) &\equiv \frac{\langle \hat{a}_1^\dagger(0)\hat{n}_d(\tau)\hat{a}_1(0)\rangle}{\langle \hat{n}_1 \rangle} \\ &= \bar{n}_d + \frac{\mathcal{T}\bar{n}_d}{4\bar{n}_1}\left[\frac{\lambda_2}{\lambda_1}e^{-2\lambda_1\tau} + \frac{\lambda_1}{\lambda_2}e^{-2\lambda_2\tau}\right]. \end{aligned} \tag{22}$$

Here, the first index denotes the port of measurement and the second index denotes the conditioning port. Thus, for example, a_{d1} is the DPO field amplitude conditioned on a detection at port 1. The third term in $n_{11}(\tau)$ arises due to interference between the CO and the DPO *conditioned* on a first photodetection at port 1.

There are several noteworthy features of these equations. First, unlike the steady-state field amplitude $\bar{a}_d$ which vanishes, the conditional DPO field amplitude $a_{d1}(\tau)$ is nonzero. Consequently, the conditional interference term in Eq. (21) is also nonzero. Second, even when the mean DPO light intensity is very small compared to the CO light intensity, the conditional interference term can cancel the contributions from the first two terms in Eq. (21). This means the fringe visibility can be nearly unity even when the two interfering fields have very dissimilar intensities. This is impossible

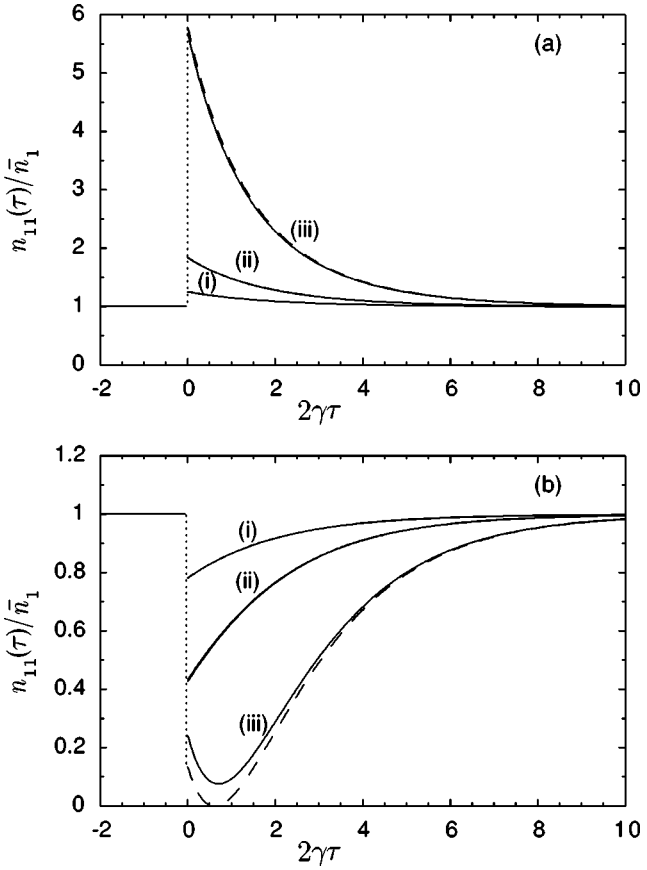

FIG. 2. Conditioned mean intensity $n_{11}(\tau)/\bar{n}_1$ at port 1 as a function of scaled time $2\gamma\tau$ for (a) $\phi=0$ and (b) $\phi=\pi/2$ for several different values of the ratio $(\bar{n}_\alpha\mathcal{R}/\bar{n}_d\mathcal{T})=600$ (i); 200 (ii); 50 (iii). For both figures $\bar{n}_d=10^{-4}$ and $\bar{n}_1$ is the steady-state mean photon number for port 1. The dashed curves represent the coherent result $|a_{11}(\tau)/\bar{n}_1|^2$ for the same parameters. The times before $\tau=0$ correspond to the steady state.

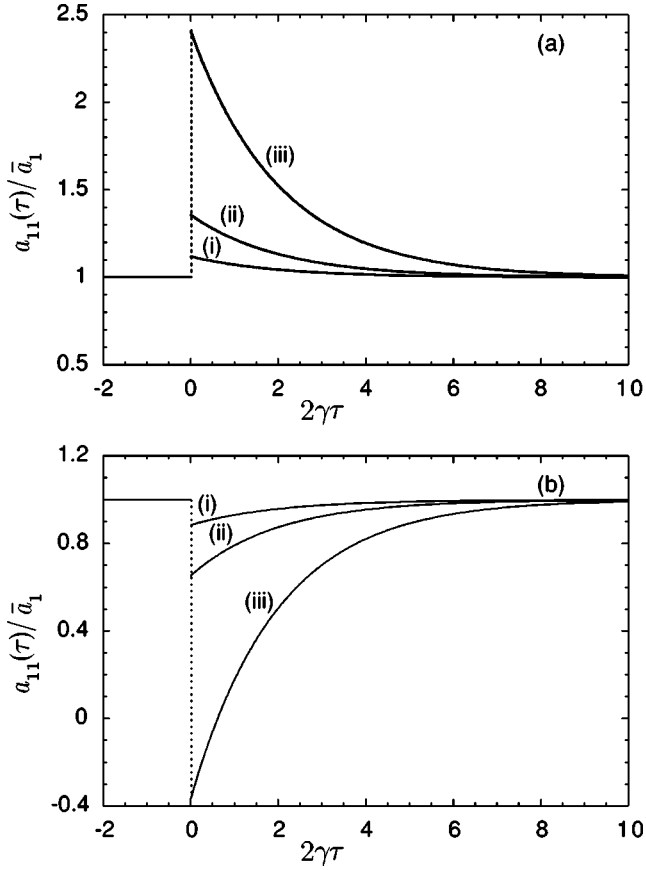

FIG. 3. Conditioned mean-field amplitude $a_{11}(\tau)/\bar{a}_1$ at port 1 as a function of scaled time $2\gamma\tau$ for (a) $\phi=0$ and (b) $\phi=\pi/2$ for several different values of the ratio $(\bar{n}_\alpha\mathcal{R}/\bar{n}_d\mathcal{T})=600$ (i); 200 (ii); 50 (iii). For both figures $\bar{n}_d=10^{-4}$ and $\bar{a}_1$ is the steady-state field amplitude at port 1. The times before $\tau=0$ correspond to the steady state.

with classical sources. Figures 2(a) and 2(b) show plots of intensity $n_{11}(\tau)$ for several different values of the ratio $\mathcal{R}\bar{n}_\alpha/\mathcal{T}\bar{n}_d$. For $\phi=0$ [Fig. 2(a)], the intensity shows an enhancement immediately after a first detection and thereafter monotonically relaxes to its steady-state value. For $\phi=\pi/2$, on the other hand, the behavior of $n_{11}(\tau)$ can be nonmonotonic as seen in Fig. 2(b). For example, the curve labeled (iii) shows that the conditioned intensity decreases first before turning around and relaxing toward its steady-state value. Another noteworthy feature is that the curves in Fig. 2(b) violate one or more of the classical inequalities $n_{11}(0)\geqslant\bar{n}_1$, $n_{11}(0)\geqslant n_{11}(\tau)$, $|n_{11}(0)-\bar{n}_1|\geqslant|n_{11}(\tau)-\bar{n}_1|$. These inequalities follow from those satisfied by the second-order intensity correlation function [13–18]. This nonclassical behavior of conditioned intensity arises due to a nonclassical interference of the conditioned DPO field with the CO field as will be seen shortly [8].

Unlike the steady-state emission, the conditional emission from the DPO has a definite phase relative to the CO. From Eq. (20), the phase ψ of the DPO field immediately after a first photodetection is given by

$$\tan\psi=-\tan\phi\left(\frac{\gamma-\kappa\varepsilon}{\gamma+\kappa\varepsilon}\right). \tag{23}$$

Far below threshold ($\kappa\varepsilon\ll\gamma$), this gives $\psi\approx-\phi$. Thus, if a first photodetection occurs with phase ϕ, the DPO radiates with phase $-\phi$. Figures 3(a) and 3(b) show the time evolution of the superposed field amplitude at port 1 over an interval during which a first photodetection occurs. The superposed field amplitude has been normalized so that its steady state value is unity. Before detection the system is in the steady-state and the superposed field amplitude has the mean $\bar{a}_1=\sqrt{\mathcal{R}}\alpha$. After a photodetection, the mean-field amplitude changes abruptly from the steady-state value $\sqrt{\mathcal{R}}\alpha$ to the value given by Eqs. (19) and (20),

$$a_{11}(0)=\sqrt{\mathcal{R}}\alpha+\frac{\mathcal{T}\bar{n}_d}{\bar{n}_1}\left(\alpha+\frac{\gamma}{\kappa\varepsilon}\alpha^*\right). \tag{24}$$

For $\phi=0$ [Fig. 3(a)], this amplitude is real and positive. In this case, the DPO field amplitude adds to the CO field amplitude resulting in an enhanced amplitude immediately after

a photodetection. It then monotonically relaxes to its steady-state value. This is consistent with Fig. 2(a) for the intensity.

For $\phi=\pi/2$ [Fig. 3(b)], the conditioned field amplitude $a_{11}(0)$ is pure imaginary. The contribution from the second term in Eq. (24), which represents the conditional field from the DPO, can become negative imaginary. The mean-field radiated by the DPO is zero before detection [Eq. (8)] and changes discontinuously to $a_{d1}(0)=\sqrt{\mathcal{RT}}(\bar{n}_d/\bar{n}_\alpha)[\alpha+(\gamma/\kappa\varepsilon)\alpha^*]$ [Eq. (20)]. For small $\bar{n}_d$ (which implies $\gamma/\kappa\varepsilon>>1$) and $\phi=\pi/2$, the conditioned DPO field amplitude is $a_{d1}(0)\approx\sqrt{\mathcal{RT}}(\gamma\bar{n}_d/\kappa\varepsilon|\alpha|^2)\alpha^*=-\sqrt{\mathcal{RT}}(\gamma\bar{n}_d/\kappa\varepsilon|\alpha|^2)\alpha$. Thus, after the detection of the first photon, the field radiated by the DPO is out of phase with the laser field at port 1. It subtracts from the CO contribution and, depending on the operating point of the DPO and the ratio $\mathcal{T}\bar{n}_d/\mathcal{R}\bar{n}_\alpha$, it can cancel the CO field amplitude. It can even exceed the CO field, thereby changing the sign of the overall field amplitude as seen in Fig. 3(b) [curve labeled (iii)]. Following the detection, the field amplitude relaxes along the imaginary axis back to the steady state according to Eqs. (19) and (20). If after a first detection the field amplitude becomes negative, then during its passage to the steady state it passes through zero at some nonzero delay [curve (iii) in Fig. 3(b)]. If the state of the superposed field after a photodetection were a coherent state, the conditioned mean intensity of the superposed field at port 1 would be

$$n_{1c}(\tau)\equiv|a_{11}(\tau)|^2=\bar{n}_1\left[\cos^2\phi\left(1+\frac{\kappa\varepsilon\mathcal{T}e^{-\lambda_1\tau}}{\bar{n}_1}\frac{}{2\lambda_1}\right)^2+\sin^2\phi\left(1-\frac{\kappa\varepsilon\mathcal{T}e^{-\lambda_2\tau}}{\bar{n}_1}\frac{}{2\lambda_2}\right)^2\right]. \quad (25)$$

This function vanishes whenever $a_{11}(\tau)$ vanishes. The dashed curves in Fig. 2 representing the normalized coherent intensity $n_{1c}(\tau)/|\bar{a}_1|^2$ are seen to be good approximation to the exact conditional intensities (continuous curves). The difference in the exact intensity and the coherent result near the minimum is due to the incoherent fluctuations of the DPO represented by the second term in Eq. (22). The importance of this term decreases as $\bar{n}_d$ becomes smaller. For $\bar{n}_d\ll1$, the coherent result $n_{1c}(\tau)$ is a good approximation to the conditioned photon number $n_{11}(\tau)$. In this limit, therefore, we can speak of the DPO field amplitude having a definite phase as in a coherent state.

It is also remarkable that for the parameters of Fig. 2, the CO field is much stronger than the DPO field ($\mathcal{R}\bar{n}_\alpha\gg\mathcal{T}\bar{n}_d$), yet the field radiated by the DPO can cancel or even exceed the CO field. We have already noted that the enhanced conditioned emission from the DPO is rooted in the creation of photon pairs inside the DPO cavity. When the first photon of a pair is detected the conditioned mean photon number for the DPO increases temporarily and the DPO emits at an enhanced rate such that the second photon leaks out within a time $(2\gamma)^{-1}$ of the first.

Induced coherence after a first detection is also reflected in the conditioned mean photon number of the $\hat{a}_2$ mode. A

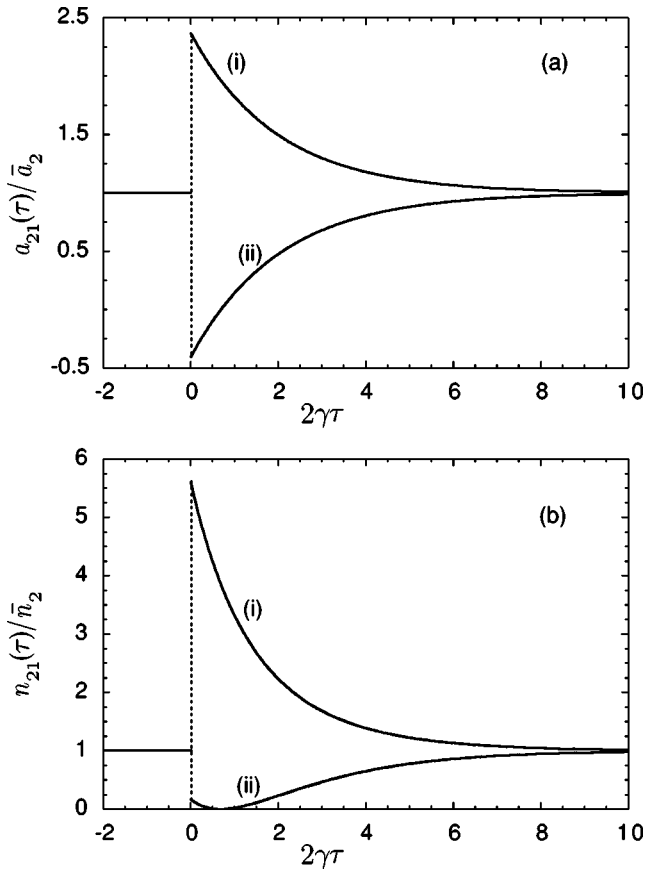

FIG. 4. Conditioned mean-field amplitude $a_{21}(\tau)/\bar{a}_2$ (a) and intensity $n_{21}(\tau)/\bar{n}_2$ (b) at port 2 as functions of scaled time $2\gamma\tau$ for (i) $\phi=\pi/2$ and (ii) $\phi=0$. The curves are for $\mathcal{R}=\mathcal{T}$, $\bar{n}_d=10^{-4}$, $(\bar{n}_\alpha\mathcal{R}/\bar{n}_d\mathcal{T})=50$. $\bar{a}_2$ and $\bar{n}_2$ are the steady-state amplitude and intensity at port 2.

calculation similar to the one outlined here shows that the relevant averages for the $\hat{a}_2$ mode are given by

$$a_{21}(\tau)\equiv\frac{\langle\hat{a}_1^\dagger(0)\hat{a}_2(\tau)\hat{a}_1(0)\rangle}{\langle\hat{n}_1\rangle}=\sqrt{\mathcal{T}}\alpha-\sqrt{\mathcal{R}}a_{d1}(\tau), \quad (26)$$

$$n_{21}(\tau)\equiv\frac{\langle\hat{a}_1^\dagger(0)\hat{n}_2(\tau)\hat{a}_1(0)\rangle}{\langle\hat{n}_1\rangle}=\mathcal{T}\bar{n}_\alpha+\mathcal{R}n_{d1}(\tau)-\sqrt{\mathcal{RT}}[\alpha a_{d1}^*(\tau)+\alpha^*a_{d1}(\tau)]. \quad (27)$$

Using these equations together with Eq. (20), we see that immediately following a photodetection at port 1 the conditional contribution from the DPO to mode $\hat{a}_2$ is with phase $\pi-\phi$. Figures 4(a) and 4(b) show the time evolution of conditional amplitude $a_{21}(\tau)$ and photon number $n_{21}(\tau)$.

For $\phi=\pi/2$, the conditional field radiated by the DPO interferes destructively with the CO field at port 1 and constructively at port 2. In this case, the interference term in $n_{21}(\tau)$ reinforces the contribution from the first two terms. This is shown by the curves labeled (i) in Figs. 4(a) and 4(b). By comparing the behavior of $n_{11}(\tau)$ and $n_{21}(\tau)$, we find

that while the conditional probability of detecting a photon at port 1 is negligible, the probability of detecting a photon at port 2 is high.

For $\phi=0$ [curve (ii) in Fig. 4(a)], we find that the conditioned field from the DPO interferes destructively at port 2 and constructively at port 1 [Fig. 4(b)]. Figure 4(b) shows the time evolution of $n_{21}(\tau)$ in this case. We see that while the conditional probability of detecting a photon at port 2 is negligible, the corresponding probability of detecting a photon at port 1 is high [Fig. 2(b)]. The dip in n_{21} for $\phi=0$ [Fig. 4(b), curve (ii)] arises due to the fact that in this case the DPO field contribution at port 2 is out of phase with the CO field and exceeds its magnitude. The overall conditional amplitude at port 2 therefore changes sign immediately following the first detection [curve (ii) in Fig. 4(a)]. As the amplitude a_{21} relaxes toward its steady-state value, it crosses zero at some finite time. This is reflected in the behavior of $n_{21}(\tau)$ as a function of time [Fig. 4(b), curve (ii)]. The dashed curves in Fig. 4(b) representing $|a_{21}(\tau)/\bar{a}_2|^2$ are indistinguishable from the exact intensities. This once again reinforces coherent nature of emission from the DPO especially for small $\bar{n}_d$.

The asymmetry between ports 1 and 2 implied by Figs. 2 and 4 is not due to the asymmetric beam splitter BS_1 (beam reflected from the upper face suffers a phase change of π relative to that reflected from the lower face) in Fig. 1. For example, for $\phi=\pi/4$, we find that $n_{11}(\tau)$ and $n_{21}(\tau)$ decreases monotonically for $\tau>0$ and there is very little difference between them. Indeed it can be checked that by considering other types of beam splitters, we arrive at the same results albeit for different values of ϕ. Quantities such as $n_{22}(\tau)$ and $n_{12}(\tau)$ that are conditioned on a first photodetection at port 2 can be similarly discussed but do not lead to qualitatively new phenomena. In particular, for the special case $\mathcal{R}=\mathcal{T}=1/2$, we find $n_{11}(\tau)=n_{22}(\tau)$ and $n_{12}(\tau)=n_{21}(\tau)$.

Finally, we consider the effect of unequal reflectivity and transmittivity of the beam splitter. An inspection of $n_{11}(\tau)$ shows that it depends only on $\bar{n}_d$ and the ratio $\mathcal{R}\bar{n}_\alpha/\mathcal{T}\bar{n}_d$. On the other hand, $n_{21}(\tau)$ depends on these two variables and also explicitly on the ratio $\mathcal{T}/\mathcal{R}$. For a fixed $\bar{n}_d$, when we vary $\mathcal{R}$ (with $\mathcal{R}+\mathcal{T}=1$), the ratio $\mathcal{R}\bar{n}_\alpha/\mathcal{T}\bar{n}_d$ can be kept constant by adjusting $\bar{n}_\alpha$. We then find that as $\mathcal{R}$ is varied by keeping $\bar{n}_d$ and $\mathcal{R}\bar{n}_\alpha/\mathcal{T}\bar{n}_d$ constant, $n_{11}(\tau)$ remains unchanged but $n_{21}(\tau)$ changes. This is shown in Fig. 5. As $\mathcal{R}$ is varied from 0.4 to 0.6 the shape of $n_{21}(\tau)$ changes. This dependence of $n_{21}(\tau)$ on $\mathcal{T}/\mathcal{R}$ can be utilized to tailor the intensity at port 2 following a detection at port 1.

It is clear that the phase of the conditioned field from the DPO plays an important role. This phase can be detected by a homodyne setup. For example, if we take the efficiencies of detectors D_1 and D_2 to be the same and BS_1 to be a 50:50 ($\mathcal{R}=\mathcal{T}=1/2$) beam splitter, the difference signal conditioned on a photodetection at port 1 is

$$n_{11}(0)-n_{21}(0)=\frac{\bar{n}_\alpha\bar{n}_d}{\bar{n}_1}\left[1+\frac{\gamma}{\kappa\varepsilon}\cos 2\phi\right]. \tag{28}$$

Thus, if phase ϕ is modulated the conditioned difference signal will contain a modulation at twice the frequency. As ϕ deviates from $\pm\pi/2$ and approaches 0, the nonclassical features in $n_{11}(\tau)$ and $n_{12}(\tau)$ are gradually washed out. They would be revealed, however, rather dramatically in a measurement that we describe next.

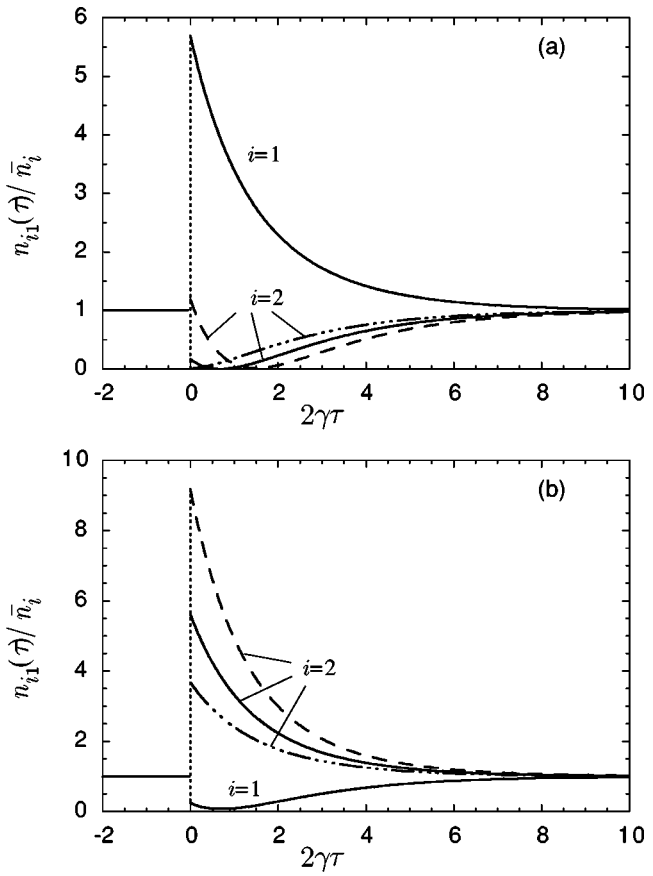

FIG. 5. Effect of unequal beam splitter reflectivity and transmittivity on the intensities at the two ports for (a) $\phi=0$, (b) $\phi=\pi/2$. The curves are for fixed values of $\bar{n}_d=10^{-4}$ and $(\bar{n}_\alpha\mathcal{R}/\bar{n}_d\mathcal{T})=50$, and for $\mathcal{R}=0.5$ (—); $\mathcal{R}=06$ (- - -); and $\mathcal{R}=0.4$ $-\cdots-$.

III. CONDITIONAL MEASUREMENTS OF QUADRATURE FLUCTUATIONS

It is well known that the quadrature fluctuations of the field emitted by the DPO exhibit nonclassical squeezing. Quadrature variables for the DPO can be introduced by

$$\hat{X}_{d\theta}=\frac{1}{2}(e^{-i\theta}\hat{a}_d+e^{i\theta}\hat{a}_d^\dagger), \tag{29}$$

$$\hat{Y}_{d\theta}=\frac{1}{2i}(e^{-i\theta}\hat{a}_d-e^{i\theta}\hat{a}_d^\dagger), \tag{30}$$

where the phase θ is arbitrary. Note that $\hat{Y}_{d\theta}=\hat{X}_{d\theta+\pi/2}$. For the DPO both quadratures have zero mean and their normally ordered variances are given by

$$\langle:(\Delta\hat{X}_{d0})^2:\rangle=\frac{1}{4}\frac{\kappa\varepsilon}{\lambda_1}, \tag{31}$$

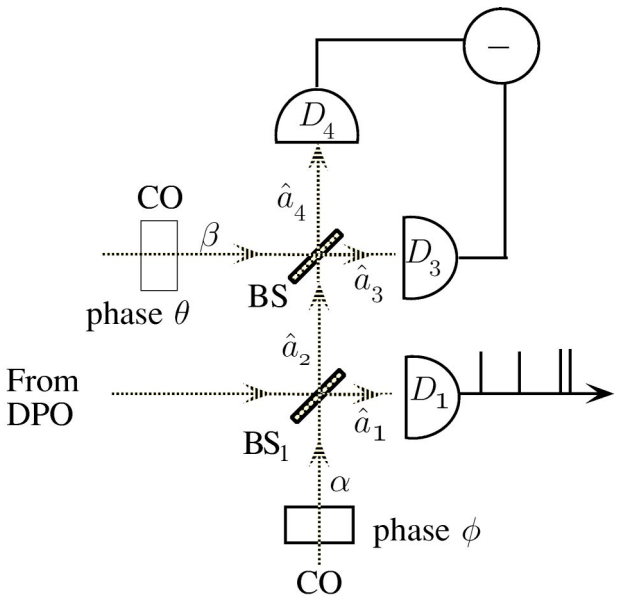

FIG. 6. A setup for balanced homodyne detection of mode $\hat{a}_2$. BS is a 50:50 beam splitter. This arrangement replaces the detector D_2 in Fig. 1.

$$\langle{:}(\Delta\hat{Y}_{d0})^2{:}\rangle = -\frac{1}{4}\frac{\kappa\varepsilon}{\lambda_2}. \tag{32}$$

For classical fields these fluctuations are always positive. Since normally ordered variance of quadrature $\hat{Y}_{d0}$ for the DPO becomes negative its fluctuations are squeezed indicating their nonclassical character. Fluctuations of quadrature $\hat{X}_{d0}$, on the other hand, stay positive as would be the case for a classical field. They are, nevertheless, nonclassical and their nonclassical character is revealed in a conditional measurement made by using the arrangement outlined in Fig. 6. For this purpose, we have replaced the second detector D_2 in Fig. 1 by a homodyne detection setup for the beam exiting port 2 of the beam splitter BS_1. The beam exiting the second port is mixed with another coherent field of amplitude $\beta = |\beta| e^{i\theta}$ at a "50:50" beam splitter BS. The fields at the two outputs of this beam splitter will be given by

$$\hat{a}_3 = \frac{1}{\sqrt{2}}(\beta + \hat{a}_2), \tag{33}$$

$$\hat{a}_4 = \frac{1}{\sqrt{2}}(-\beta + \hat{a}_2). \tag{34}$$

A balanced homodyne measurement of $\hat{a}_2$, conditioned upon a photodetection of mode $\hat{a}_1$ at $\tau = 0$ is given by [3]

$$F(\tau,\theta,\phi) = \frac{\langle{:}\hat{a}_1^\dagger(0)[\hat{n}_3(\tau) - \hat{n}_4(\tau)]\hat{a}_1(0){:}\rangle}{\overline{n_1}}, \tag{35}$$

where the mean photon number $\overline{n_1} = \langle \hat{a}_1^\dagger \hat{a}_1 \rangle$ for mode $\hat{a}_1$ is given by Eq. (18) and we have explicitly taken into account the fact that $\hat{a}_1$ depends on ϕ and $\hat{a}_3$ and $\hat{a}_4$ depend on θ. Using Eqs. (33) and (34) for $\hat{a}_3$ and $\hat{a}_4$, together with Eqs. (15) and (16) for $\hat{a}_1$ and $\hat{a}_2$, we find

$$F(\tau,\theta,\phi) = \frac{2|\alpha||\beta|\sqrt{\mathcal{T}}}{\overline{n_1}}[-2\mathcal{R}\langle{:}\hat{X}_{d\phi}(0)\hat{X}_{d\theta}(\tau){:}\rangle + \cos(\phi-\theta)\overline{n_1}]. \tag{36}$$

By choosing the photon number for mode $\hat{a}_1$ to be $\overline{n_1} \equiv \mathcal{R}|\alpha|^2 + \mathcal{T}\overline{n_d} = 2\mathcal{R}\overline{n_d}$, which can always be done by adjusting the coherent field photon number so that $|\alpha|^2 = \overline{n_d}[2 - (\mathcal{T}/\mathcal{R})]$ and by setting $\theta = \phi$, we obtain

$$F(\tau,\phi,\phi) = \frac{4|\alpha||\beta|\mathcal{R}\sqrt{\mathcal{T}\overline{n_d}}}{\overline{n_1}}\left[-\frac{\langle{:}\hat{X}_{d\phi}(0)\hat{X}_{d\phi}(\tau){:}\rangle}{\overline{n_d}} + 1\right]. \tag{37}$$

This function depends on the quadrature correlation function $\langle{:}\hat{X}_{d\phi}(0)\hat{X}_{d\phi}(\tau){:}\rangle$. In the limit $\tau \to \infty$, this correlation function factorizes and vanishes because $\langle \hat{X}_{d\phi}\rangle = 0$. In this limit, the function $F(\tau,\phi,\phi)$ reaches the value

$$F_\infty \equiv \frac{4|\alpha||\beta|\mathcal{R}\sqrt{\mathcal{T}\overline{n_d}}}{\overline{n_1}}. \tag{38}$$

Using this value, we introduce a normalized function

$$f_\phi(\tau) \equiv \frac{F(\tau)}{F_\infty} = \left[-\frac{\langle{:}\hat{X}_{d\phi}(0)\hat{X}_{d\phi}(\tau){:}\rangle}{\overline{n_d}} + 1\right], \tag{39}$$

which characterizes conditional quadrature fluctuations. This correlation function satisfies certain inequalities. These inequalities are easily derived by noting that for a field $\hat{a}$, with quadrature operators $\hat{X}_\phi = (e^{-i\phi}\hat{a} + e^{i\phi}\hat{a}^\dagger)/2$ and $\hat{Y}_\phi = (e^{-i\phi}\hat{a} - e^{i\phi}\hat{a}^\dagger)/2i$, the amplitude and quadrature fluctuations are related by

$$\langle{:}\Delta\hat{a}^\dagger\Delta\hat{a}{:}\rangle = \langle{:}(\Delta\hat{X}_\phi)^2{:}\rangle + \langle{:}(\Delta\hat{Y}_\phi)^2{:}\rangle, \tag{40}$$

where for an operator $\hat{O}$ the quantity $\Delta\hat{O} = \hat{O} - \langle\hat{O}\rangle$. Dividing both sides of Eq. (40) by $\langle{:}\Delta\hat{a}^\dagger\Delta\hat{a}{:}\rangle$, we obtain

$$1 = \frac{\langle{:}(\Delta\hat{X}_\phi)^2{:}\rangle}{\langle{:}\Delta\hat{a}^\dagger\Delta\hat{a}{:}\rangle} + \frac{\langle{:}(\Delta\hat{Y}_\phi)^2{:}\rangle}{\langle{:}\Delta\hat{a}^\dagger\Delta\hat{a}{:}\rangle}. \tag{41}$$

For classical fields $\langle{:}(\Delta\hat{X}_\phi)^2{:}\rangle$, $\langle{:}(\Delta\hat{Y}_\phi)^2{:}\rangle$, and $\langle{:}\Delta\hat{a}^\dagger\Delta\hat{a}{:}\rangle$ are all positive quantities. It follows that the fluctuations of both quadratures satisfy the inequality

$$0 \leqslant \frac{\langle{:}(\Delta\hat{X}_\phi)^2{:}\rangle}{\langle{:}\Delta\hat{a}^\dagger\Delta\hat{a}{:}\rangle} \leqslant 1. \tag{42}$$

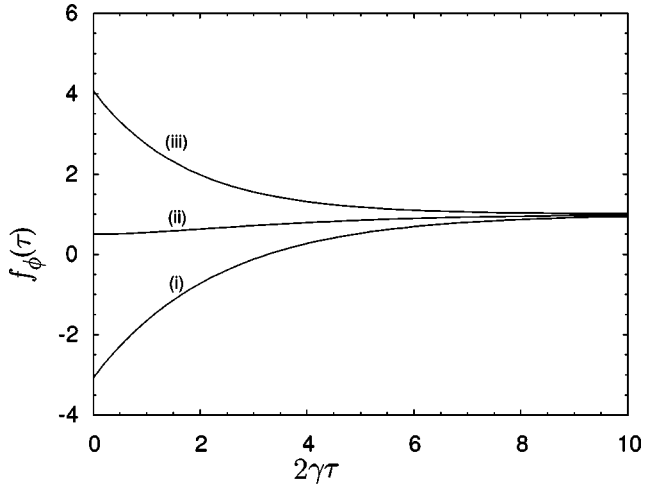

FIG. 7. Plots of $f_\phi(\tau)$ for $\bar{n}_d=10^{-2}$ and $\phi=0$ (i); $\pi/4$ (ii); $\pi/2$ (iii). $f_\phi(0)<0$, $f_\phi(0)>1$, or $f_\phi(\tau)<f_\phi(0)$ indicate nonclassical behavior.

Using Schwartz inequality, we can also establish the following bound satisfied by classical fields:

$$\frac{\langle:[\Delta\hat{X}_\phi(0)]^2:\rangle}{\langle:\Delta\hat{a}^\dagger\Delta\hat{a}:\rangle}\geqslant\frac{\langle:\Delta\hat{X}_\phi(0)\Delta\hat{X}_\phi(\tau):\rangle}{\langle:\Delta\hat{a}^\dagger\Delta\hat{a}:\rangle}. \tag{43}$$

If the mean value of the field amplitude and quadratures vanish, then with the help of these inequalities we find that the function $f_\phi(\tau)$ for a classical field satisfies the inequalities

$$0\leqslant f_\phi(0)\leqslant 1, \tag{44}$$

$$f_\phi(\tau)\geqslant f_\phi(0). \tag{45}$$

Using the relation between quadrature and annihilation and creation operators, we find the correlation function needed to calculate $f_\phi(\tau)$ for the DPO field is

$$\frac{\langle:\hat{X}_{d\phi}(0)\hat{X}_{d\phi}(\tau):\rangle}{\langle:\hat{a}_d^\dagger\hat{a}_d:\rangle}=\frac{\kappa\varepsilon}{4\bar{n}_d}\left[\frac{e^{-\lambda_1\tau}}{\lambda_1}\cos^2\phi-\frac{e^{-\lambda_2\tau}}{\lambda_2}\sin^2\phi\right]. \tag{46}$$

We note that $f_\phi(\tau)$ for $\phi=0$ depends on unsqueezed quadrature fluctuations [Eq. (31)] and for $\phi=\pi/2$ it depends on squeezed quadrature fluctuations [Eq. (32)]. The results for the DPO in the two cases are

$$f_0(\tau)=1-\frac{\kappa\epsilon}{4\bar{n}_d\lambda_1}e^{-\lambda_1\tau}, \tag{47}$$

$$f_{\frac{\pi}{2}}(\tau)=1+\frac{\kappa\epsilon}{4\bar{n}_d\lambda_2}e^{-\lambda_2\tau}. \tag{48}$$

These functions are plotted in Fig. 7. We see that both $f_0(\tau)$ and $f_{\pi/2}(\tau)$ violate the inequality (44) that restricts classical fluctuations of both quadratures, as characterized by $f_\phi(0)$, to be bounded by 0 and 1. Nonclassical character of squeezed quadrature fluctuations is already revealed in unconditioned measurements as noted following Eq. (32). Measurements of f_ϕ reveal not only the nonclassical character of the squeezed quadrature fluctuations but also of the unsqueezed quadrature fluctuations. The violation of classical inequalities in terms of f_ϕ can be rather large. For example, below threshold ($\kappa\varepsilon\ll\gamma$, $\bar{n}_d\ll 1$), we find

$$f_0(0)\approx 1-\frac{1}{2\sqrt{2\bar{n}_d}}\ll -1,\quad f_{\pi/2}(0)\approx 1+\frac{1}{2\sqrt{2\bar{n}_d}}\gg 1. \tag{49}$$

Thus, the fluctuations of both quadratures exhibit giant violations of classical inequality (44). We also note that $f_{\pi/2}(\tau)$ for the squeezed quadrature violates not only the first inequality (44) but also the second inequality (45). In addition to revealing the nonclassical character of both quadrature fluctuations f_ϕ has another advantage. By virtue of its normalization in Eq. (39), the function $f_\phi(\tau)$ is largely independent of the efficiency of detection. This is in contrast to the usual homodyne detection of squeezing that is degraded by nonunit detector efficiency.

It is also noteworthy that nonclassical features of the field revealed in $f_\phi(\tau)$ are most pronounced when $\bar{n}_\alpha=\bar{n}_d$ (for $\mathcal{R}=\mathcal{T}$), whereas those revealed in n_{ij} are usually most pronounced when $\bar{n}_d/\bar{n}_\alpha\ll 1$. In this sense, the two ways of characterizing nonclassical fluctuations are complementary. Time evolution of $n_{ij}(\tau)$ and $f_\phi(\tau)$ reflects the dynamical evolution of the intensity and quadrature variables following a detection. Conditional measurements coupled with the freedom provided by ϕ allow us to select the "correct" phase for observing nonclassical excursions of fluctuations.

IV. SUMMARY

In this paper, we have considered conditional measurements as probes of quantum dynamics. Such measurements not only provide a deeper understanding of nonclassical features of quantum dynamic but also lead to different ways of characterizing them. By taking a degenerate parametric oscillator operating below threshold as a model system, we have given quantitative analytic results that can be tested in photoelectric counting experiments. Our results show that the nonclassical intensity correlations of the DPO are a consequence of enhanced coherent emission from the DPO after a first photodetection. Our approach reveals that like squeezed quadrature fluctuations unsqueezed quadrature fluctuations are also nonclassical. Whereas unconditional measurements reveal only the nonclassical character of squeezed quadrature fluctuations, conditional measurements reveal the nonclassical character of both quadrature fluctuations and in much more dramatic manner than unconditional measurements.

The features of quantum mechanics that most distinguish

it from classical mechanics are the interference of probability amplitudes and entanglement. Conditional measurements allow us to probe these nonclassical features of quantum dynamics for a degenerate parametric oscillator and provide different ways of understanding and revealing the nonclassical character of quantum fluctuations.

ACKNOWLEDGMENTS

This work was supported in part by the Office of Naval Research and the Arkansas Science and Technology Authority. D.E. and S.S. acknowledge support from the ICSC World Laboratory.

[1] H.J. Carmichael, *An Open Systems Approach to Quantum Optics* (Springer-Verlag, Berlin, 1993); H.J. Carmichael, S. Singh, R. Vyas and P.R. Rice, Phys. Rev. A **39**, 1200 (1989).

[2] L. Mandel and E. Wolf, Rev. Mod. Phys. **37**, 231 (1965); D.F. Walls, Nature (London) **306**, 141 (1983); R. Loudon, Rep. Prog. Phys. **43**, 913 (1980).

[3] H.J. Carmichael, H.M. Castro-Beltran, G.T. Foster, and L.A. Orozco, Phys. Rev. Lett. **85**, 1855 (2000).

[4] G.T. Foster, L.A. Orozco, H.M. Castro-Beltran, and H.J. Carmichael, Phys. Rev. Lett. **85**, 3149 (2000).

[5] M. Wolinsky and H.J. Carmichael, Phys. Rev. Lett. **60**, 1836 (1988).

[6] R. Vyas and S. Singh, Phys. Rev. A **40**, 5147 (1989); Opt. Lett. **14**, 1110 (1989).

[7] R. Vyas, Phys. Rev. A **46**, 395 (1992); R. Vyas and S. Singh, Phys. Rev. Lett. **74**, 2208 (1995).

[8] H. Deng, D. Erenso, R. Vyas, and S. Singh, Phys. Rev. Lett. **86**, 2770 (2001).

[9] R.G. Smith, in *Optical Parametric Oscillators and Amplifiers*, edited by F.T. Arecchi and E.O. Schulz-Dubois, Laser Handbook Vol. I (North-Holland, Amsterdam, 1972), p. 837.

[10] *The Physics of Quantum Information*, edited by D. Bouwmeester, A. Ekert, and A. Zeilinger (Springer-Verlag, Berlin, 2000); M.A Nielsen and I.L. Chuang, *Quantum Computation and Quantum Information* (Cambridge University Press, New York, 2000); H.-K. Lo, S. Popescu, and T. Spiller, *Introduction to Quantum Computation and Information* (World Scientific, Singapore, 1998).

[11] L. Mandel and E. Wolf, *Optical Coherence and Quantum Optics* (Cambridge University Press, New York, 1995), pp. 36–38.

[12] A. Yariv, *Quantum Electronic* (Wiley, New York, 1989), Chap. 17.

[13] A.B. Dodson and Reeta Vyas, Phys. Rev. A **47**, 3396 (1993).

[14] P.W. Milonni and S. Singh, Adv. At., Mol., Opt. Phys. **28**, 75 (1991).

[15] H.J. Carmichael, R.J. Brecha, and P.R. Rice, Opt. Commun. **82**, 73 (1991).

[16] R. Vyas and S. Singh, J. Opt. Soc. Am. B **17**, 634 (2000).

[17] P.R. Rice and H.J. Carmichael, IEEE J. Quantum Electron. **24**, 1351 (1988).

[18] L. Mandel, Phys. Scr., T **12**, 34 (1986).